Eur Biophys J (1991) 20:165–176

European Biophysics Journal

The quantal gating charge of sodium channel inactivation

N. G. Greeff and I. C. Forster

Physiologisches Institut, Universität Zürich-Irchel, Winterthurer Strasse 190, CH-8057 Zürich, Switzerland

Received April 8, 1991/Accepted in revised form June 3, 1991

Abstract. Using a very low noise voltage clamp technique it has been possible to record from the squid giant axon a slow component of gating current (I_g) during the inactivation phase of the macroscopic sodium current (I_{Na}) which was hitherto buried in the baseline noise. In order to examine whether this slow I_g contains gating charge that originates from transitions between the open (O) and the inactivated (I) states, which would indicate a true voltage dependence of inactivation, or whether other transitions contribute charge to slow I_g, a new model independent analysis termed isochronic plot analysis has been developed. From a direct correlation of I_g and the time derivative of the sodium conductance dg_{Na}/dt the condition when only O-I transitions occur is detected. Then the ratio of the two signals is constant and a straight line appears in an isochronic plot of I_g vs. dg_{Na}/dt. Its slope does not depend on voltage or time and corresponds to the quantal gating charge of the O-I transition (q_h) divided by the single channel ionic conductance (γ). This condition was found at voltages above -10 mV up to $+40$ mV and a figure of 1.21 e^- was obtained for q_h at temperatures of 5 and 15 °C. At lower voltages additional charge from other transitions, e.g. closed to open, is displaced during macroscopic inactivation. This means that conventional Eyring rate analysis of the inactivation time constant τ_h is only valid above -10 mV and here the figure for q_h was confirmed also from this analysis. It is further shown that most of the present controversies surrounding the voltage dependence of inactivation can be clarified. The validity of the isochronic plot analysis has been confirmed using simulated gating and ionic currents.

Key words: Sodium channel – Gating current – Inactivation – Voltage dependence

Introduction

The initial time course of the action potential in nerve or muscle is determined mainly by the voltage dependent activation or opening of the membrane sodium channels (Hodgkin and Huxley 1952; Hille 1984). A further inherent property of this channel is its subsequent inactivation which leads to an additional closed state and ensures the termination of the action potential. Both processes occur faster at higher membrane potentials. The voltage dependence of such gating processes is thought to originate from the displacement of electrically charged amino-acids within the channel protein, thereby providing a link between membrane voltage and conformational change (Armstrong 1981). These charge displacements, although consisting of small quanta per conformational transition, build up to a measurable macroscopic gating current when the average frequency of these transitions is sufficiently large (Armstrong and Bezanilla 1977; Keynes and Rojas 1976). This is illustrated in Fig. 1 which shows schematically the different signals generated by Na channels when voltage clamped to depolarizing potentials (V_p). These are the macroscopic sodium current (I_{Na}) which has been shown to be the sum of the microscopic currents (i_{Na}) from many stochastically operating single channels (Sigworth and Neher 1980). In addition there is the macroscopic gating current (I_g), but here the corresponding quantal events from single channel gating currents (i_g) have so far been too small for direct recording. They are assumed to be short current shots (Conti and Stühmer 1989) with a fixed charge quantum for a specific transition of the order of one electronic equivalent charge (e^-) in contrast to the single channel ionic currents where several thousand ions per millisecond pass the membrane. The size of such i_g quanta is conventionally estimated indirectly by the Eyring rate analysis (Rojas and Keynes 1975; Bezanilla 1985). In contrast to the activation process, con-

Abbreviations: I_g – gating current; I_{Na} – sodium ionic current; g_{Na} – macroscopic sodium conductance; γ – single channel conductance; C, O, I – closed, open, inactivated state occupancy of channels; q_h – quantal charge displaced in a single O-I transition of Na channel; e^- – equivalent electron charge; h – index referring to inactivation process; S_l – limiting slope in isochronic plot, see Eq. (3); δ – fractional distance, see Fig. 4 and (4, 5); TMA – tetramethylammonium; TTX – tetrodotoxin; Tris – tris(hydroxymethyl)aminomethane; HEPES – N-2-hydroxyethylpiperazine-N′-2-ethanesulfonic acid

Offprint requests to: N. G. Greeff

siderable uncertainty surrounds the very existence of the voltage dependence of the microscopic inactivation and the size of its quantal charge q_h (shaded in Fig. 1), as discussed with the aid of Fig. 1 below. It is this issue which is specifically addressed in this paper and quantitatively clarified using new methodical approaches.

In the first successful formal description of the macroscopic sodium current of the squid giant axon by Hodgkin and Huxley (1952), inactivation was assumed to be an independent gating mechanism, parallel to activation. From the analysis of the voltage dependence of the macroscopic inactivation time constant τ_h, and from the so-called steady state inactivation parameter (h_∞) they deduced a value for q_h for the transition from the open (O) to the inactivated (I) states of about $3\,e^-$. For many years the general belief was that channels would pass relatively rapidly through several closed states (C) to the open state and then during the decline of the macroscopic I_{Na} only the slower inactivation transitions O-I would occur, closing the channels as depicted in Fig. 1 B. This picture seemed to have been changed completely by recordings from single channel Na currents from mammalian neurons (Aldrich et al. 1983; Aldrich and Stevens 1987). At potentials below -20 mV it was observed that activation transitions (C-O) occurred quite often during the late phase of macroscopic inactivation and also reopenings were observed (Vandenberg and Horn 1984) before finally reaching the absorbing I-state as depicted in Fig. 1 A (C-O-C-O-I). The mean open time of these events was found to be voltage independent in contrast to the macroscopic τ_h over the voltage range of -60 to -30 mV (Aldrich and Stevens 1987). This led to the view that the macroscopic τ_h gains most of its voltage dependence indirectly via the activation rate, i.e. channels would open earlier at higher voltages leading to earlier inactivation transitions and shorter τ_h's even with nearly voltage independent O-I transitions. The quantal inactivation charge q_h was estimated to be as little as $0.3\,e^-$ (Aldrich and Stevens 1987). This trend of attributing the voltage dependence of the apparent τ_h to the C-O transition was taken further and q_h was even assumed to be zero also at higher voltages (e.g. Gonoi and Hille 1987; Catterall 1988). Different views, however, came from other single channel studies (Vandenberg and Horn 1984) where recordings at higher potentials seemed to indicate a change of the behaviour as shown in Fig. 1 A to the one in Fig. 1 B and q_h was found to be larger than $0.3\,e^-$. (It has to be noted that single channel currents are more difficult to record at higher potentials since the kinetics become faster, and closer to the sodium reversal potential the amplitude becomes smaller). From squid axon experiments a value of $0.6\,e^-$ for q_h was estimated in order to explain that the macroscopic peak conductance at higher voltages becomes constant, which would be difficult to explain unless both C-O and O-I transitions were voltage dependent (Stimers et al. 1985).

Thus it appears that from applying rate analysis to ionic currents alone, very divergent conclusions about the magnitude of q_h or the voltage dependence of inactivation respectively can be drawn, and are still accepted (see Discussion). In the present paper we exploit once more the

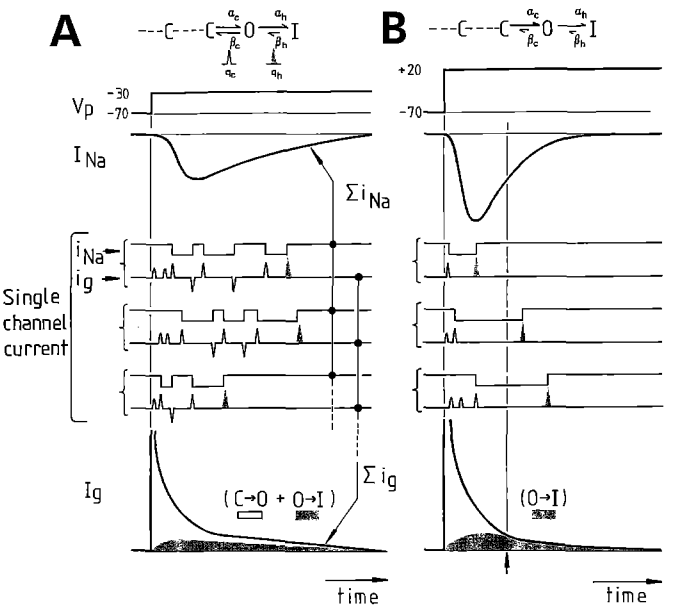

Fig. 1. Schematic representation of signals generated by Na channels when voltage-clamped to two different voltage steps (V_p) illustrating for -30 mV (**A**) and $+20$ mV (**B**) two hypothetical cases with respect to the processes during the inactivation phase (see text). Main emphasis is given to the transitions between the open (O), the inactivated (I) and the last closed state (C) while preceding closed states are not regarded relevant in this context. Sequential state diagrams at the top define the nomenclature used here for the rate constants between states and the quantal displacement (gating) charges per single transition q_C or q_h respectively. The quantal i_g from C-O or O-I transitions would coincide with the opening or closing time respectively as seen in the single channel ionic current i_{Na}, while C-C transitions would only show up in the i_g but not the i_{Na} trace. Note that single channels might undergo forward but also backward transitions. The macroscopic gating current I_g, however, from a large number of channels is only in one direction and appears as a smooth signal like the macroscopic ionic current I_{Na}. Polarity of gating current is upward for transitions from left to right in state diagram. The putative O-I gating current is shaded in the single channel traces i_g and the macroscopic I_g, and other gating charge is unshaded

macroscopic gating current I_g that has been measured for over 15 years in squid. I_g has a relatively large amplitude during the fast activation phase but during the later time course of macroscopic inactivation the signal disappeared in the baseline noise in squid (e.g. Armstrong and Bezanilla 1977); some slow I_g components were reported in crayfish by Swenson (1983) and from the node of Ranvier by Meves and Pohl (1990). Recently we have developed a technique to obtain very low noise recordings of gating current from the squid giant axon (Bekkers et al. 1986 b; Forster and Greeff 1990) and have now succeeded in detecting a slow component also during the inactivation phase. This allows the direct analysis of gating current for the estimation of the inactivation gating charge. To do this, a new analytical approach is presented here which can enable one to investigate whether this slow and small component of I_g consists of only q_h contributions as shown in Fig. 1 B or is contaminated by q_c quanta from C-O transitions as shown in Fig. 1 A or might even consist of only q_c quanta, as discussed above, if q_h were zero. Using this technique, which involves interpretation of an

isochronic plot of the amplitudes of gating current versus the time derivative of the ionic conductance, strong evidence for the voltage dependence of the actual inactivation transition is found and an estimate for q_h of about $1.2\,e^-$ is obtained. The isochronic plot analysis also indicates the voltage range and time interval during the inactivation phase, over which the decay of the ionic current is determined by the O-I transition alone. It becomes evident that τ_h is controlled by the O-I transition only above about -10 mV and during the later phase of inactivation and otherwise depends on C-O transitions as well. Much of the above mentioned controversy, therefore, seems to result from using rate analysis in a limited voltage region and extrapolating the conclusions beyond this range. Clarifying the voltage dependence of inactivation appears relevant also to separate it from the activation process such that the latter may be analysed better in the future. An accurate estimation of q_h, i.e. a single gating transition will also be valuable when testing hypotheses about this process in molecular mechanical terms. Short accounts of our results have been presented in abstract form (Forster and Greeff 1989; Greeff and Forster 1990).

Theory: Isochronic plot analysis

The method of the isochronic analysis differs from conventional approaches using rate analysis in that it does not attempt to fit exponentials to time-varying data. Instead, the relation between the amplitudes of sodium ionic current and of gating current is investigated and time is eliminated. The principle of the method is developed in a semi-analytical way based on Fig. 1. This approach seems justified, because before knowing the exact nature of the sodium channel gating process, a full analytical treatment is not possible and would also unneccessarily complicate the understanding of the principle. A further consolidation and justification of the method will be given in the Discussion by means of a full simulation and analysis of some commonly used models.

Suppose first that late in the inactivation phase, all channels have left the closed state(s) and, as shown in Fig. 1 B after the vertical marker, only O-I transitions occur. Then the following relations are readily derived, where $N_0(t)$ denotes the number of channels in the open state which varies with time, and $dN_0(t)/dt \equiv N_0(t)'$. The gating current $I_g(t)$ would then be given by the product of the rate of open channels disappearing into the inactivated state $N_0(t)'$ and the charge quantum q_h that is contributed by each O-I transition,

$$I_g(t) = -N_0(t)' \cdot q_h + \left\{\begin{array}{l} -(\text{C-O}) \cdot q_c \\ -\text{other transitions C-C, C-I} \\ -\text{other contaminations} \end{array}\right\} \quad (1)$$

and the terms in brackets of (1) are for the present purposes neglected.

On the other hand the macroscopic sodium conductance $g_{Na}(t)$ (equal to $I_{Na}/(V_p - V_{Na})$, V_{Na} being the Na-reversal potential) is always equal to the product of the number of open channels $N_0(t)$ and the constant single channel conductance γ. Differentiating this relationship gives:

$$-g_{Na}(t)' = -N_0(t)' \cdot \gamma. \quad (2)$$

Comparison of (1) and (2) shows that the two experimentaly obtainable quantities $I_g(t)$ and $-g_{Na}(t)'$ vary over time such that their ratio is always constant under the above assumption of only O-I transitions occurring. Dividing (1) by (2) gives:

$$-I_g(t)/g_{Na}(t)' = q_h/\gamma = S_l \quad (3)$$

where the ratio S_l is a constant and independent of time and voltage. Alternatively, an isochronic plot of $I_g(t)$ against $-g_{Na}(t)'$ should yield a straight line with a limiting slope S_l, as shown below. At earlier times I_g is larger owing to transitions other than O-I (terms in brackets of (1)) and $-g_{Na}(t)'$ is smaller owing to opening channels, and so the isochronic ratio is larger than S_l.

Turning to the case shown in Fig. 1 A it shall now be investigated whether there might be other conditions which produce a straight line but with an I_g containing contaminating terms as indicated in brackets in (1). Here C-O transitions occur late during the macroscopic inactivation phase and the macroscopic slow I_g is a mixture of q_c and q_h quanta. This might occur at lower voltages where the forward and backward rate constants α_c and β_c of the C-O transition are such that a channel may open again before it finally inactivates according to the inactivation rate constant α_h. Theoretical considerations show (see Discussion) that it may well happen that the (C-O) $\cdot$ q_c amplitude during macroscopic inactivation has the same time course as the (O-I) $\cdot$ q_h amplitude (i.e. same Eigenvalues). The ratio of (3) would then also yield a constant, i.e. an isochronic straight line but with a slope that is larger than the limiting slope S_l. The important point here is that at higher voltages α_c grows while β_c becomes smaller such that the open state is reached more quickly and the channels will more likely undergo an O-I transition instead of returning to the C-state. Hence the q_c contribution in I_g will decrease relative to the q_h contribution and the ratio $-I_g(t)/g_{Na}(t)'$ will asymptote to the limiting slope S_l.

Note that similar considerations can be applied for other contaminating gating currents from e.g. C-C or C-I transitions and that any specific state diagram for the gating process can be examined and compared with the experimental data as shown in the Discussion.

In summary, the procedure to detect O-I gating currents is as follows:

1) Search in the isochronic plot of $I_g(t)$ against $-g_{Na}(t)'$ for a straight line during the late phase of macroscopic inactivation (expect possibly straight lines with larger slopes at lower voltages).

2) Find the voltage range where these straight lines have the same voltage independent limiting slope S_l, which then corresponds to q_h/γ.

Material and methods

The resolution of any putative inactivation gating current necessitates a high recording signal-to-noise ratio. Our

recordings were made using an improved version of a cylindrical axon voltage clamp from 5 mm lengths of the cylindrical membrane of a squid axon (*Loligo forbesii*) with diameters ranging between 800 and 1000 μm. Based on our previous estimate of the sodium channel density as 180 per μm^2 (Bekkers et al. 1986a) one then records gating current from about $2.5 \cdot 10^9$ channels providing a large signal. About a 10-fold reduction of the system noise was achieved by a balanced improvement of the major noise sources (Bekkers et al. 1986b; detailed description Forster and Greeff 1990). Since the inactivation gating current is expected to be a relatively slow process (time constants around 1 to several ms) special care was also taken to reduce slow baseline fluctuations. We also found it essential to perfuse the axon with a solution that replaces potassium ions by TMA^+ (tetramethylammonium) for at least 30 to 60 min in order to block any ionic leak current through the potassium channels almost perfectly. As discussed later, this protocol should also eliminate potassium gating current.

Experimental chamber and voltage clamp

Freshly dissected axons were cannulated and perfused by a dialysis tube (Bullock and Schauf 1978) and placed in a temperature and solution controlled chamber. Salient features of the low noise clamp are: *i)* From a 5 mm length of axon in the central pool the membrane current was measured using a low noise Op-amp (LT 1028, Linear Technology) configured as virtual ground current-to-voltage converter; *ii)* the central pool was partly separated using perspex partitions from the 6.5 mm long guard pools on either side held at ground potential; this decreased the current-noise generating shunt conductance from the I/V converter to ground from about 0.1 S to 0.01 S; *iii)* a special piggy back triple electrode measured the internal voltage in the center of chamber via a KCl filled 60 μm glass capillary DC-coupled to an Ag-AgCl wire, and in parallel via a 25 μm Pt wire that extended from an insulating glass capillary by about 2 mm providing by additional Pt-coating a large surface, low resistance voltage sensor which was AC-coupled to the AgCl electrode in order to block slowly changing polarization potentials. *iv)* The differential amplifier of the clamp was of discrete design using at the input low noise FETs (a chip made of dual 50 parallel FETs type 2SK146, Toshiba) and gave an equivalent input voltage noise density of 2.5 $nV/Hz^{1/2}$. The overall signal to noise improvement was 8 to 10 fold compared to our previous design.

I_{Na} recordings were performed after allowing for enough perfusion time to ensure that stable Na reversal potential (E_{rev}) was defined by internal and external $[Na^+]$. Filter frequency of usually 10 kHz (6-pole Bessel) was identical to I_g recording as also the leak and capacity transient subtracting pulses from -80 mV to -130 mV alternating with the forward pulses from a holding potential of -80 mV up to $+60$ mV in steps of 10 mV. The low $[Na]_{ext}$ and at least 70% series resistance (R_s)-compensation minimised errors due to R_s. Recordings of gating current with little averaging for subtraction of I_g in I_{Na} records followed after TTX block.

The high resolution I_g recordings were sometimes done on the same axons as for I_{Na} but often on fresh axons in order to obtain optimal recordings. The following optimizations for slow I_g were used: The back-reference pulse for capacity transient and leak subtraction was chosen between -80 mV to -130 mV since this was found to cause very little droop of baseline in contrast to the usual $-150/-180$ mV and we checked that it did not introduce any gating current during the inactivation time window. 50 Hz contaminations that were still visible after the usual precautions at this signal scale were eliminated by use of 50 Hz locked sampling, and after each pulse a trace at holding potential containing the contamination was sampled and subtracted. Usually 64 averages were taken at 2 temperatures of 5 or 15 °C. Currents were measured per membrane area as obtained from the axon diameter. The correlation of I_g and I_{Na} taken at different axons was further corrected if necessary by comparing the initial I_g amplitude in the I_{Na} record and I_g proper.

Solutions: In m*M* external: 103 NaCl, 413 *Tris*-Cl, 55 $CaCl_2$, 11 $MgCl_2$; for I_g all Na replaced by *Tris* and 1 μ*M* tetrodotoxin (TTX) added; internal: 20 NaF, 330 tetramethylammonium (TMA^+) fluoride, 400 sucrose, 10 Hepes; for I_g 350 TMA, 0 Na; pH 7.2 at 5 °C. The voltage pulses to and the current signal from the voltage clamp were sampled by an analog/digital interface (CED-502, Cambridge Electronic Design) interfaced to a LSI 11/73 (Digital Equipment) computer. Programs for the experimental protocols and the analysis were written in DAOS-6.0, and for some part of the analysis in the equivalent PC-AT version, DAOS-7.1 (Mycon Technology, Melbourne, Australia).

Results

Gating current during macroscopic inactivation of I_{Na}

Figure 2A, C shows sodium ionic currents I_{Na} and high resolution gating currents I_g as recorded under identical conditions using 10 kHz filter bandwidth and a transient subtraction pulse between -80 and -130 mV at 5 °C. From a series of pulse potentials from -60 to $+60$ mV in steps of 10 mV and a holding potential of -80 mV the recordings for pulses to 0 mV and $+30$ mV are shown. In the scaled-up trace of I_g one can see a signal that roughly parallels the inactivation of I_{Na} but has only an amplitude well under 1 $\mu A/cm^2$ compared to about 30 $\mu A/cm^2$ for the peak activation gating current (note that the peak of the gating current is rounded and smaller in comparison to high bandwidth recordings due to the filter action; it has been verified that the slow I_g is not affected). The pulse for the gating current lasted throughout the entire sampling period of 40 ms in order to check for any droop in the baseline which is absent in this experiment.

At first we used conventional kinetic analysis and fitted multiple exponentials to the data. But this turned out to be difficult with respect to quantifying the slow gating current and no convincing correlation between I_g and the inactivation phase could be obtained (Keynes et al. 1990). This might be partly due to the observation that the fitting procedure is extremely sensitive to even slight fluctu-

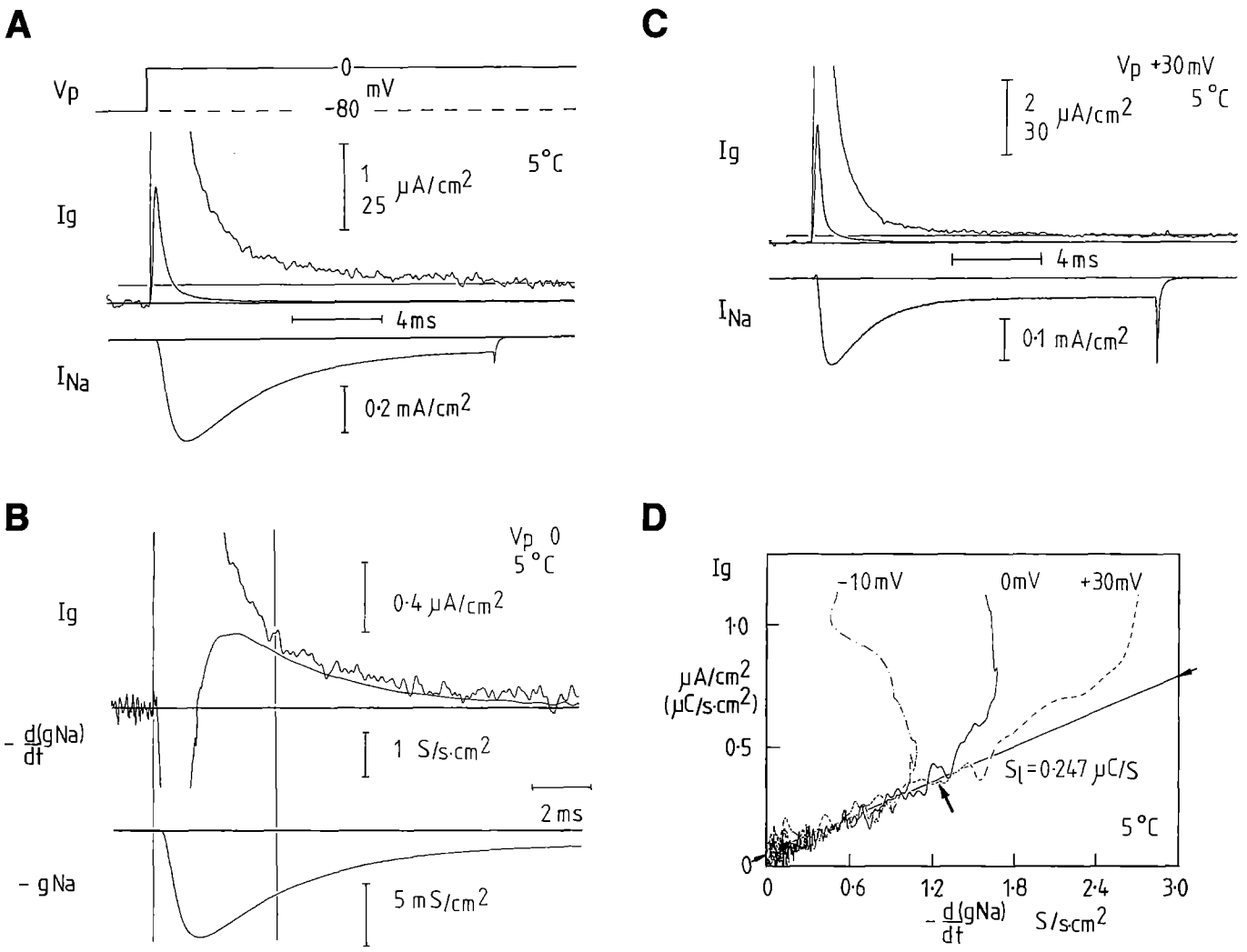

Fig. 2 A–D. Gating current I_g and ionic current I_{Na} of sodium channels recorded from a voltage clamped squid giant axon at two test potentials V_p of 0 and +30 mV and illustration of the isochronic plot analysis at 5 °C. **A** $V_p = 0$ mV; I_g is shown on 2 scales showing the peak during activation and the small gating current during inactivation of I_{Na} which is displayed on the same time scale (I_{Na} pulse lasting only 15 ms). I_g was recorded during 40 ms in order to obtain the baseline level after the end of sodium inactivation (not shown); the small constant level of leak current found in this record is indicated by the thin horizontal line and subtracted in further analysis. **B** Data from A; I_g baseline adjusted to 0 and on larger scale ($\mu A/cm^2 = \mu C/s \cdot cm^2$); ionic current converted to conductance $g_{Na} = I_{Na}/(V_p - V_{Na})$ ($V_{Na} = 48$ mV) shown negative as its time derivative $-dg_{Na}/dt$ given in S(iemens)/(s · cm²). **C** Same as **A** but for $V_p = +30$ mV showing faster kinetics. Note the constant baseline in I_g after the end of inactivation; not all sodium channels inactivate due to incomplete inactivation (Chandler and Meves 1970b) especially in TMA^+ and at higher V_p; the dg_{Na}/dt signal will, however, only arise from inactivating channels. **D** Isochronic plot of signals in **B**, i.e. I_g vs. $-dg_{Na}/dt$ during the decay of inactivation. The large arrow marks for $V_p = 0$ mV the time given by vertical line in **B**. Straight line, indicated by small arrows is fitted by eye and has a slope of 0.247 µC/S. Expts. K14O and K17O

ations in the baseline. Also the unknown overlap of activation and inactivation might cause difficulties in separating kinetic entities within an arbitrarily chosen time window. Therefore we adopted the strategy of applying the isochronic analysis to the late phase of inactivation where a putative O-I gating current would be less contaminated.

Application of isochronic analysis to the experimental data

Figure 2 B shows the same recordings as in Fig. 2 A for a testpulse to 0 mV and addition the time derivative of $I_{Na}(t)$ as needed for our analysis. It can be seen that $I_g(t)$ and $-g_{Na}(t)'$ indeed appear to decline in equal proportion for times later than that marked by the vertical line. This is more easily seen in the isochronic representation in Fig. 2 D where the two signals after the marked time clearly follow a straight line. Before that time the ratio $-I_g(t)/g_{Na}(t)'$ is larger. Figure 2 C shows the time course of both signals at $V_p = +30$ mV. It is clearly seen that the inactivation proceeds much faster than at $V_p = 0$ mV but in the isochronic representation in Fig. 2 D a straight line with the same slope as at $V_p = 0$ is obtained. According to the above theory this means that this slope is the limiting slope $S_l = q_h/\gamma$ and that at these voltages and, as also shown down to −10 mV, an appreciable part of the later inactivation phase is given by the O-I transition alone,

corresponding to the hypothesis in Fig. 1 B. Otherwise one would expect a change of the slope at the different voltages.

A systematic isochronic analysis over a wide voltage range from − 20 to + 40 mV is shown in Fig. 3 for the two temperatures of 5 and 15 °C. Only at − 20 mV and below (not shown) is there a suggestion of a linear segment in the small and noisy signals with a steeper slope of about 0.4 to 0.6 μC/S and higher consistent with the behaviour discussed above for lower voltages. Above + 40 mV close to the reversal potential the sodium currents with the sodium concentrations used become small and $g_{Na}(t)'$ becomes contaminated by noise and is therefore not shown. Otherwise at both temperatures with different kinetics, one finds for voltages above − 10 mV satisfactory superpositions of straight lines with slopes of 0.247 μC/S at 5 °C and 0.180 μC/S at 15 °C. The different slopes S_l at the two temperatures give a Q_{10} of 0.180/0.247 equal to 1/1.37. This would be expected according to our theory which gives $q_h = S_l \cdot \gamma$ from (3). The single channel conductance γ has a Q_{10} of 1.3 resulting from ion diffusion in water and this figure has been confirmed experimentally for single sodium channels by Nagy et al. (1983). Thus taking the temperature dependencies of S_l and γ together implies that q_h is temperature independent. This is consistent with the idea that only the rate constants associated with conformational changes have a temperature dependence but not the quantal charge displaced since the size of the intramolecular conformational displacement per gating transition should be independent of rate, voltage and temperature. It is the advantage of the isochronic analysis that it eliminated time and measures gating charge per conductance change. At this state of the analysis the observed superimposing slopes indicate, at both temperatures, the constraints with respect to voltage and time where inactivation is controlled by the same gating charge quantum related to the O-I transition. This conclusion can be drawn even before knowing the size of q_h, which is quantified below.

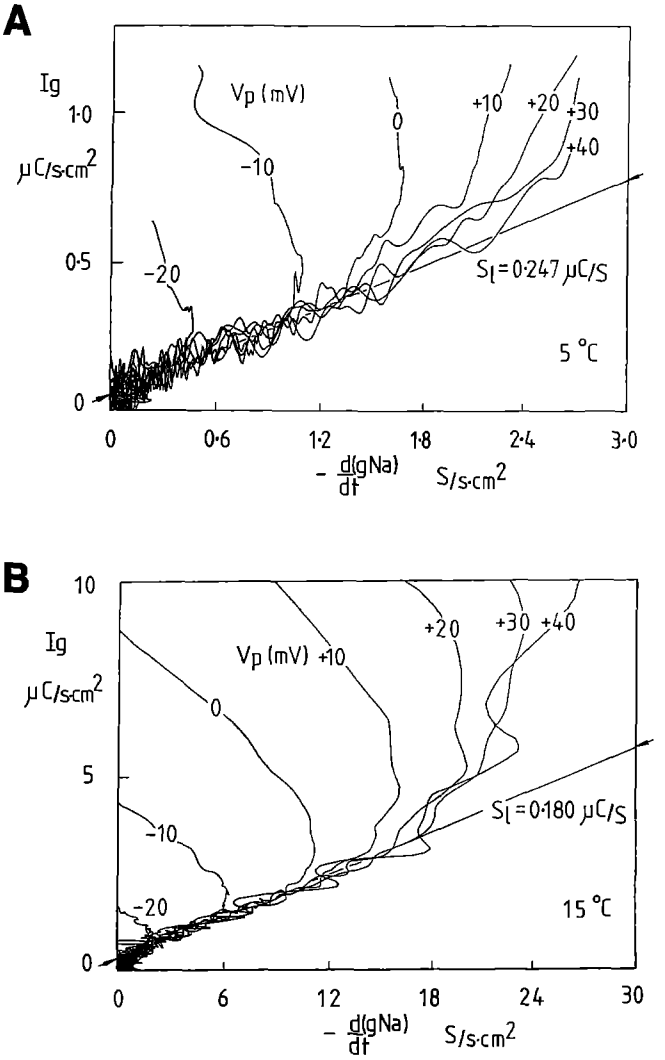

Fig. 3. Isochronic plots of I_g vs. $-dg_{Na}/dt$ for test pulses from −20 mV to +40 mV in steps of 10 mV as indicated at **A** for 5 °C and **B** for 15 °C. Traces obtained as in Fig. 1. The constant baseline level measured at the far end of the pulse was subtracted from I_g traces at 5 °C; at 15 °C the baseline showed a slight linear droop and a sloping baseline fitted after the end of inactivation was subtracted (this procedure changed the slope S_l by less than 4%). A simple 3-point digital filter was applied to all signals to reduce the peakiness of high frequency noise. The common slope indicated by the eye fitted straight line S_l (ends marked by arrows) is 0.247 μC/S at 5 °C and 0.180 μC/S at 15 °C. Expts. K17O, K5N, K14O

Estimation of quantal charge

For the calculation of q_h an accurate value of γ under the same experimental conditions is needed. It should be noted that γ depends more or less on several experimental conditions: *i*) temperature; *ii*) internal and external sodium concentrations; *iii*) the concentration of external divalent cations such as Ca^{++} and Mg^{++} that are high in seawater and may reduce γ by factors of up to 8 according to single channel studies from the cut-open squid axon by Bezanilla (Yamamoto et al. 1984; Bezanilla 1987). (This probably accounts for most of the difference of γ observed in mammalian sodium channels compared to those in marine animals). Under the present conditions γ would be too small for single channel recording but we have measured it using non-stationary fluctuation analysis, in an earlier extensive series of experiments (Bekkers et al. 1986a) on the same preparation including the identical conditions used in the present study except that Cs^+ perfusion was used. In the course of changing from Cs^+ to TMA^+ perfusion we have also determined that the conductance of the sodium channels in TMA^+ is 71% of that in Cs^+ and have confirmed using instantaneous current-voltage steps that γ is voltage independent in Cs^+ and TMA^+ up to the reversal potential. This has been tacitly assumed above but would otherwise of course lead to voltage dependent slopes, S_l.

Table 1 gives the estimates for q_h at both temperatures from the data of 4 experiments which each covered the complete voltage range and were minimally affected by leak or baseline droop. Each figure for S_l represents the mean of one V_p family of superimposing slopes (− 20 mV to +40 mV, steps of 10 mV). The variation at different test potentials within a V_p family was about ± 5%. It can

Table 1. S_l as obtained from 4 experiments (* from Fig. 2). γ is obtained from rechecking all our earlier fluctuation experiments (Bekkers et al. 1986a) and found for the exact conditions of the present experiments at 5 °C as 0.83 (±0.06) pS ($n=4$) which was further confirmed by extrapolation from experiments comparing different Na concentrations. From this estimate the value of γ at 15 °C was obtained using the Q_{10} of 1.3 for ion diffusion (also verified in single channel experiments (Nagy et al. 1983)). From (3) $q_h = S_l \cdot \gamma/(1.6 \cdot 10^{-19}\,C/e^-)$

	S_l (μC/S)	γ (pS)	$q_h(e^-)$
5 °C	0.247*	0.83	1.28
5 °C	0.220	0.83	1.14
15 °C	0.180*	1.08	1.22
15 °C	0.179	1.08	1.21
	Mean ± SD ($n=4$)	1.21 (±0.06)	

be seen that the estimates for q_h from the different experiments are rather close to the mean of $1.21 \pm 0.06\,e^-$ (SD, $n = 4$) at both temperatures. One should allow a ± 10% tolerance for the absolute value resulting from the effects of small baseline artifacts that cannot be treated in detail here.

Comparison with Eyring rate analysis

Having now learned from the isochronic analysis the conditions under which the macroscopic inactivation time constant is determined by only the O-I transition, the traditional estimation of q_h may now be reexamined. According to the Eyring rate theory (Rojas and Keynes 1975; Bezanilla 1985) the rate constants α (forward) and β (backward) and the apparent time constant τ in the macroscopic signal of a transition with a charge displacement q depend on voltage V as follows:

$$\alpha = \alpha_0 \exp[q\,V\,\delta/kT] \quad (4)$$

$$\beta = \beta_0 \exp[-q\,V\,(1-\delta)/k\,T] \quad (5)$$

$$\tau = 1/(\alpha + \beta) \quad (6)$$

k is Boltzmann's constant, T absolute temperature and α_0, β_0 are the rates at 0 mV. Note, as detailed under Fig. 4, that α and β depend not on the full size of q but on the fraction δ or $(1-\delta)$ respectively. This corresponds to the fractional distance between one of the stable states or energy wells to the position of the energy barrier peak when q moves along the electric field. The q thus determined corresponds to an effective charge which would be transferred across the whole field or the entire membrane respectively. The physical charge might be larger but then transferred only across a corresponding fraction of the field (see Discussion). Two critical points have to be considered when assessing the result of a rate analysis. Firstly is has to be ensured that the apparent time constants are controlled by the rate constants of one conformational transition only, otherwise the estimation of q from the measured τ/V relation will be in error (see simulation in Discussion). Secondly it should be noted that it is unclear in many investigations whether the resulting q of a rate

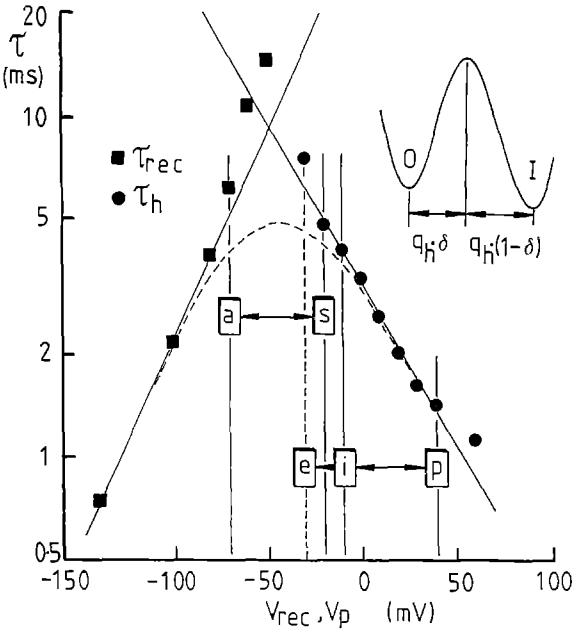

Fig. 4. Eyring rate analysis of sodium current inactivation. The *insert* shows the free energy profile associated with the Eyring rate equations (4, 5) for the experimentally found rate constants (below) and their voltage dependence. An energy barrier separates the two wells at open (O) and inactivated state (I). Abscissa gives charge movement along electric field according to fractional distance δ to barrier maximum from either energy well. The *main figure* shows the logarithmic plot of inactivation time constant τ_h and recovery time constant τ_{rec} of I_{Na} against voltage at 5 °C. τ_h obtained from logplots of I_{Na}'s of experiment in Fig. 2A at indicated V_p's, confirmed also by fitting single exponentials to the decline during inactivation after the steepest gradient in I_{Na}. The straight line fitted by eye through the τ_h points at $V_p = -10$ to +40 mV gives $1/\alpha_h(V_p)$ and according to (4) its slope of 46 mV per e-fold decline gives $q_h \cdot \delta = 0.52$ electronic charges. τ_{rec} was obtained using standard double pulse protocols (Armstrong and Bezanilla 1977; Greeff et al. 1982) measuring recovery from inactivation at indicated V_{rec} (Expt. I21N). The straight line fitted by eye to points to the left where τ_{rec} should approximate $1/\beta_h$ has a steepness of 36 mV per e-fold change corresponding to $q_h \cdot (1-\delta) = 0.67$ electronic charges. Taking α_h and β_h from these fitted lines, the theoretical $\tau = 1/(\alpha_h + \beta_h)$ of the inactivation gate on its own (unaffected by e.g. activation, see text) was calculated and plotted as dashed line. The vertical thin lines **a** and **s** indicate the V_p-range of the single channel analysis by Aldrich and Stevens (1987) (see Discussion), and the lines **i** and **p** the range where the isochronic plot analysis shows a constant limiting slope corresponding to $q_h = 1.21\,e^-$; between lines **e** and **i** the isochronic slope is larger suggesting the contamination by error terms due to other transitions

analysis is taken as the full q or the fraction $q \cdot \delta$ or $q \cdot (1-\delta)$ respectively. A full analysis should determine the transitions in both directions in order to obtain α and β separately and from this both fractions of q. Often the simplifying assumption of a symmetrical energy barrier with $\delta = 0.5$ is made and only one direction analysed.

Experimentally the kinetics of the inactivation gate are measured in the forward direction (O → I; see Fig. 4) from the inactivation time constant τ_h at different voltages. For the backward direction the time constant of recovery from the inactivated state τ_{rec} as obtained with a double pulse protocol (Armstrong and Bezanilla 1977; Greeff et al. 1982) may be used under the assumption that

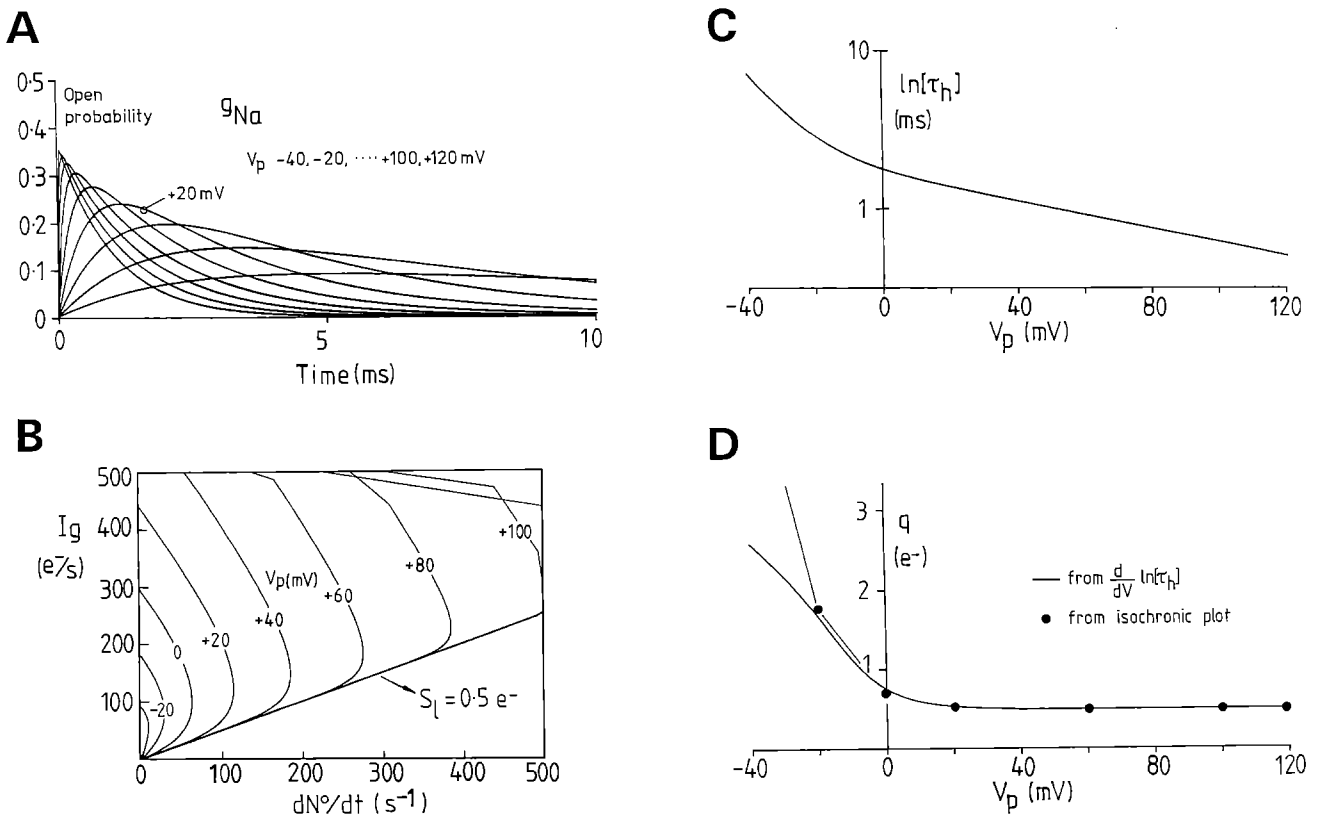

Fig. 5A–D. Simulation of isochronic analysis using a 3-state scheme (C-O-I), see discussion in text. **A** The curves for ionic conductance $g_{Na}(t)$ and $I_g(t)$ (not shown) were computed for voltages V_p −40 to +120 mV in steps of 20 mV; the quantal charges were $q_C = 2\,e^-$ for C-O and $q_h = 0.5\,e^-$ for O-I; the rate constants at 0 mV in ms^{-1} were $\alpha_c = 1\,500$ and $\beta_c = 60$, $\alpha_h = 600$ and $\beta_h = 0.4$ and for other voltages computed from (4, 5) assuming $\delta = 0.5$. **B** Isochronic representation of the $I_g(t)$ traces as a function of $-dg_{Na}(t)/dt$ given here as $-dN_O(t)/dt$ assuming single channel conductance $\gamma = 1$. **C** τ_h of macroscopic $g_{Na}(t)$ as obtained from second Eigenvalue (which is equivalent to $1/\tau_h$) continuously plotted on log scale against V_p. Note how $\ln(\tau_h)$ asymptotes to a straight line above +10 mV with an e-fold decline per 96 mV, which gives $q_h = 0.5\,e^-$ according to (4) and assuming $\delta = 0.5$. **D** Comparison of q estimation from final slope of isochronic straight line seen in **B** with estimation using rate analysis. Due to the scaling of $g_{Na}(\gamma = 1)$ the isochronic slope gives the quantal charge directly according to (3). It is clearly seen in the isochronic plot at which voltages the limiting slope is approached and the estimated q corresponds to q_h. From rate analysis of $\ln(\tau_h)$ vs. V_p the quantal charge is calculated as $2\,kT \cdot d(\ln[\tau_h])/dV_p$ (factor 2 from $\delta = 0.5$) as derived from (4) and (6) and interpreting the τ_h's to be given by only the O-I transition

at some potentials the return from the I-state dominates τ_{rec}. Although not proved here, there is good evidence for this to be so, as illustrated in a commonly used scheme (Armstrong and Bezanilla 1977; Stimers et al. 1985) that is shown here:

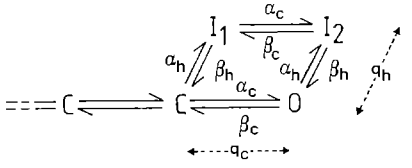

It depicts a loop, where channels activate rapidly into the O-state and from there slowly inactivate into I_2. Upon repolarisation a fast transition $I_2 \rightarrow I_1$ avoids the O-state and the slow recovery is determined by the $I_1 \rightarrow C$ transition which is slower than the C-C transitions. This is further supported by our recent findings on gating currents in the inactivated states (Bekkers et al. 1990). Both the O-I_2 and the C-I_1 transitions have the same rate constants based on the assumption that they reflect one and the same gate, which acts in parallel to the C-O or I_1-I_2 transition. If the τ's depended only on the inactivation gate they should lie on a bell shaped curve (4–6) which approaches straight lines on a log plot of τ vs. V_p on either side (dashed line in Fig. 4) where τ is either $\tau_h = 1/\alpha_h$ for $\alpha_h \gg \beta_h$ or $\tau_{rec} = 1/\beta_h$ for $\alpha_h \ll \beta_h$. Figure 4 shows τ_h and τ_{rec} vs. V_p from our data at 5 °C.

In contrast to earlier investigations it has now been deduced from the isochronic plot analysis that τ_h is controlled predominantly by the O-I transition only above − 10 mV up to the examined voltage of + 40 mV. Here τ_h should equal $1/\alpha_h$ and a straight line may legitimately be fitted through those points, the slope of which according to (4) gives the valency $q_h \cdot \delta = 0.52\,e^-$. τ_{rec} is fitted at voltages below − 100 mV assuming that here the inactivation gate is the rate limiting transition. The necessity for this assumption demonstrates the above mentioned uncertainty when using rate analysis and shall be discussed further below. Similarly, from the fitted slope to τ_{rec} we obtain $q_h(1 - \delta) = 0.67\,e^-$ and therefore $q_h = 1.19\,e^-$ and $\delta = 0.44$. Note that this estimation uses a completely different method and the good agreement with the figure for $q_h = 1.21\,e^-$ as obtained from the isochronic plot analysis, mutually corroborates the two

methods. The isochronic plot method however, is more direct because q_h is obtained simply by dividing gating charge by the number of inactivating channels, whereas in the τ/V plot one can only "a posteriori" state whether the τ's in a given voltage range should follow the theory. For example, it is observed that in the midregion the τ's are much larger than the theoretical value of $1/(\alpha + \beta)$ which is indicated by the dashed line in Fig. 4. In this voltage region the apparent τ_h is most likely controlled by both the inactivation and activation gates and their related charges. This is also apparent from the steeper slope of the isochronic curves for V_p below -10 mV (see above). Earlier estimations of q_h (see introductory paragraphs and Discussion) have often been carried out using rate analysis at voltages between 0 and -100 mV. Here the τ's depend strongly on voltage and larger estimates for q_h were obtained.

Discussion

Simulation of isochronic analysis using 3-state model

The aim of this study was not to arrive at a complete model of the sodium channel that includes activation and inactivation transitions and their coupling mode, but rather to investigate the voltage dependence of the open to inactivated (O-I) transition only (i.e. the size of the quantal charge q_h). However, a commonly used 3-state model (C-O-I) shall be simulated here in order to demonstrate that the isochronic plot analysis can detect q_h correctly. Different sets of rate constants and quantal charges for q_c (C-O) and q_h (O-I) may be chosen to generate curves for ionic conductance and gating current at different potentials. These signals are then analysed by the isochronic plot method in order to check whether the correct value for q_h can be recovered.

Figure 5 shows an example with $q_c = 2\,e^-$ and $q_h = 0.5\,e^-$ and rate constants chosen to produce typical conductance curves (Fig. 5 A). From the same simulation gating currents are obtained as resulting from q_c and q_h producing transitions which in the simulation can be separated but of course not in the experiment. The total gating current $I_g(t)$ is then plotted vs. the time derivative of the conductance $g_{Na}(t)'$ which equals dN_0/dt when the single channel conductance is taken as unity in the simulation. In this isochronic plot (Fig. 5 B) it can be seen that at low potentials at -40 and -20 mV isochronic straight lines appear but with slopes that decrease with growing V_p and approach the limiting slope from above only for $V_p \geq +20$ mV. In the simulated data it can be seen that the steeper slopes below 0 mV are caused by q_c plus q_h gating current while in the limiting slope S_l the q_c contribution is negligibly small. It may be relevant to note that this behaviour is not readily seen from analytical expressions where the formal equations contain both components. The limiting slope gives $0.5\,e^-$ for q_h which confirms the validity of the isochronic plot method.

Figure 5 C demonstrates that the macroscopic τ_h shows the behaviour predicted by the Eyring rate theory (4–6) only above $+10$ mV. Here the log τ_h vs. V_p curve is a straight line with the correct slope whereas below $+20$ mV the τ's are too large. Note that the voltage where the change occurs ($+10$ mV) depends on the rate constants chosen for the simulation and must not necessarily coincide with the experimental data. Figure 5 D compares the q values obtained from the isochronic plot analysis with those from the rate analysis. It is clear that the isochronic plot procedure detects the condition where only O-I transitions occur and hence q_h may be obtained also from the rate analysis. However, if one were given only the ionic currents and their τ_h's, it may be difficult to decide whether in a chosen voltage region the observed process is controlled by only the inactivation transition. Hence, the rate analysis might result in erroneous estimates of q_h, if say, only in the limited region -40 to -20 mV a few data points for τ_h were available and would be connected by a straight line which would not deviate much from the slightly bent curve in Fig. 5 C. A q_h of about $2\,e^-$ would then be wrongly estimated. In contrast the isochronic straight lines show marked differences at these potentials (Fig. 5 B).

It was of further interest to simulate the case of $q_h = 0$ because it is often discussed whether the macroscopic inactivation gets all its voltage dependence from the C-O transition (e.g. Gonoi and Hille 1987; Catterall 1988). Then the isochronic straight lines were found to approach very clearly the limiting slope $S_l = 0$, i.e. the $q_h = 0$ condition would be detected in the experimental data. We have also simulated an extended scheme that allows direct voltage dependent transitions C-I, i.e. bypassing the O-state, and again q_h was obtained correctly. Furthermore it is evident that a parallel activation-inactivation scheme of the Hodgkin and Huxley type (Hodgkin and Huxley 1952) will allow the detection of the true q_h. Then the faster activation will terminate independently and earlier than inactivation which thereafter will alone produce gating current. In summary the isochronic analysis appears robust in detecting q_h if embedded in various models, and it would appear that also from the experimental data, where the underlying sodium channel gating mechanism is not known, the results are not subject to a misinterpretation.

Possible sources of gating current contamination

Both ionic leakage currents through potassium channels and potassium gating current would have time constants similar to sodium inactivation and might contaminate the slow gating currents. It is known that the potassium channels lose their conductance in the absence of K^+ and Cs^+ ions (Chandler and Meves 1970 a; Almers and Armstrong 1980; Gilly and Armstrong 1980). This was also the case in our experiments where K^+ was replaced by TMA^+ and only very small leak currents of unknown origin remained (Fig. 2). As noted in the Results we estimate at the present state of analysis the error to be less than 20%. Potassium gating currents have been recorded in squid, and in the most recent studies (Spires and Begenisich 1989; Augustine and Bezanilla 1990) all published recordings were done with Cs^+ in the bath or per-

fusate, probably in order to preserve the function of the K-channels. No explicit mention was made whether these gating currents would disappear without the preserving Cs^+ as suggested in the earlier studies by Almers and Armstrong (1980) and by Gilly and Armstrong (1980), but not in another study by White and Bezanilla (1985). For the following reasons, however, we regard the potassium gating current to have become negligibly small under our experimental conditions: *i*) the very good agreement of the slow gating current with the sodium conductance time over a very large voltage and temperature range would not be expected for potassium gating current. *ii*) likewise the agreement of the estimate for q_h as obtained by two essentially different methods (isochronic plot method and rate analysis); *iii*) the size of the potassium gating current has been observed to decrease in about 10 min at 20 °C after withdrawal of the preserving Cs^+ from about 500 to less than 50 electron charges/cm^2 (personal communication by Dr. T. Begenisich, 1990). In our experiments we waited 30 to 60 min at 5 °C and then obtained stable gating charges of about 220 electron charges/cm^2 (q_h of $1.2\,e^-$ times 180 channels/cm^2, the density as obtained earlier by Bekkers et al. 1986a) which was assumed to be only negligibly contaminated by potassium gating current. We have also assessed the effect of contaminating residual ionic leakage through sodium channels and have found that this would not result in the common limiting slope behaviour seen here.

Controversies concerning the voltage dependence of inactivation

Papers referred to most often in this context are the single channel studies on neuroblastoma cells by Aldrich, Corey and Stevens (1983) and Aldrich and Stevens (1987). They could measure separately the mean channel open time T_0 and the macroscopic τ_h in the potential range of -70 to -20 mV and found a constant T_0 in the narrow potential range of -60 to -30 mV, but a strongly voltage dependent τ_h. Since $T_0(V_p) = 1/(\alpha_h + \beta_c)$, i.e. depends on the rate constants of the transitions leaving the O-state either ot C or to I respectively, one would expect a bell shaped curve for T_0 vs. V_p showing straight lines in a log-plot much like the dashed line in our Fig. 4. From the isochronic analysis it was concluded that below -10 mV τ_h depends on both the C-O and the O-I transitions and only above that voltage α_h dominates over β_c, and only then T_0 should coincide with τ_h, both being equal to $1/\alpha_h$. Thus it appears very likely that the constant T_0's found by these authors were measured at the top of the bell shaped curve where little variation is to be expected in contrast to τ_h (compare our Fig. 4 with their Fig. 5 (Aldrich and Stevens 1987)). Although limited by the single channel technique to lower test voltages, these authors found an estimate for the O-I gating charge of about 0.3 to 0.46 electrical charges (their Fig. 10). This figure interpreted as $q_h \cdot \delta$, as it is also termed more clearly by Stevens (1987), is close to our $0.52\,e^-$.

A more recent study on single cardiac sodium channels by Yue et al. (1989) (their Fig. 2) covers a larger voltage range up to + 20 mV and confirms clearly the bell shaped dependence of T_0 vs. V_p, i.e. a flat region between -40 to -10 mV and a change above -10 mV showing a true voltage dependence of the O-I transition. These findings have also been corroborated by two other groups (Berman et al. 1989; Scanley et al. 1990). Other evidence for the existence of a voltage dependent O-I step has recently been reported from experiments using optical retardation methods in squid (Landowne 1990). We believe that our gating current analysis gives the most direct and accurate figure for the total q_h and shows up the importance of knowing the behaviour at different voltage ranges. The single channel studies mentioned above are the next most direct measurement, and appear to match our findings. The least direct method, that of interpreting only macroscopic sodium currents, might easily produce wrong estimates for q_h if it is not ensured that only O-I transitions are dominating. The classical analysis by Hodgkin and Huxley (1952) attributed about $3\,e^-$ to the h-gate from measurements in the range of about -100 to 0 mV (h_∞-curve) where we think C-O and O-I transitions are interacting. A recent whole-cell sodium current analysis at GH3 cells (Cota and Armstrong 1989) reports zero voltage dependence for O-I. However, the conditions of these experiments are rather different from ours, i.e. high internal sodium and reversed currents and using papain to destroy inactivation. The same cells in another extensive study by Vandenberg and Horn (1984) show practically the same voltage dependence of τ_h as we find. From their Fig. 2, a plot of $\ln(\tau_h)$ vs. V_p, one can estimate a value for $q_h \cdot \delta$ of about 0.5 to $0.8\,e^-$ in the voltage region above 0 mV. These authors also state that τ_h approaches $1/\alpha_h$ in this voltage range ($1/\beta_I$ in their terminology on p. 556), but is larger at lower voltages. A separate study of this group (Horn et al. 1984) supports further the inherent voltage dependence of the O-I transition by measuring open times of single sodium channels in GH_3 cells before and after removal of inactivation. The kinetic analysis of macroscopic sodium currents in squid (Keynes et al. 1990) was taken further by Keynes (1991) and it is also shown that the valency of the inactivation gating charge depends on the voltage range chosen and agrees with q_h as reported here and elsewhere (Greeff and Forster 1990).

In summary, the majority of experimental findings from ionic current rate analysis, even from different preparations, are in good agreement with our data, if the interpretation takes into account the constraints with respect to voltage that we find in the present study. Concerning the size of q_h it has certainly come down from $3\,e^-$ (Hodgkin and Huxley 1952) but it would not seem justified to regard it as negligibly small for two reasons. First, since rate analysis predicts only the fraction $q_h \cdot \delta$ as $0.52\,e^-$, q_h itself is around 1 to $1.2\,e^-$ and when related to putative conformational changes involving charge movements as shown below this would be significant. Second, in comparison with the total activation gating charge of around 4 to $6\,e^-$ per channel (Armstrong 1981) this process comprises several transitional steps and each may be of similar size or even smaller than q_h.

Molecular structure-function correlation

One of the main aims of estimating the quantal charge of a single gating transition is to relate it to predictions from molecular mechanical hypotheses that have now been developed (Kosower 1985; Guy and Seetharamulu 1986; Guy 1988) following the elucidation of the primary sequence of the sodium channel (Noda et al. 1984, 1986; and Salkoff et al. 1987a, b). We have tentatively performed such a correlation (Forster and Greeff 1989) assuming the helical screw mechanism for the S_4 segments (see e.g. Guy 1988; Catterall 1988). These segments are assumed to form transmembrane α-helices and carry different amounts of positively charged residues in the four domains A, B, C and D, namely 5, 5, 6 and 8, and are very homologous in different species such as electric eel, rat and drosophila (Salkoff 1987b). They are regarded as the voltage sensor regions in the protein which would undergo a helical screw turn of 60° and 4.5 Å displacement along the electrical field. From preliminary calculations assuming that the electric field would drop across a transmembrane length of 31.5 Å we find that a single transition of 4.5 Å would produce quantal displacement charges of 0.75, 0.75, 0.85 and 1.14 electron charges for the S_4 helices in the 4 domains above, respectively (Forster and Greeff 1989). Experimental evidence from site directed mutagenesis experiments (Stühmer et al. 1989) suggests that $S_{4,A}$ is involved in activation. The quantum of inactivation gating charge of $1.21\,e^-$ obtained in the present study would best mach with $S_{4,D}$ ($1.14\,e^-$) as the voltage sensor for inactivation. Also involved in the inactivation mechanism seems to be a cytoplasmic portion or loop of the protein since inactivation can be eliminated by various drugs or enzymes acting from the inside (see reviews Hille 1984; Catterall 1988; Guy 1988). Evidence from mutagenesis experiments shows that the cytoplasmic loop between domains C and D is involved in inactivation (Stühmer et al. 1989). Previously, this finding has been used to lend support to the hypothesis of voltage independent inactivation which would be caused by a "ball and chain" hanging into the cytoplasm where it would not sense the transmembrane electric field (Armstrong and Bezanilla 1977; Armstrong 1981). Experimental evidence for such a cytoplasmic part of a channel protein which actuates the inactivation process has recently been found for the potassium channel encoded by the *Drosophila shaker* gene (Hoshi et al. 1990). However, in our opinion it would be premature to suggest as the authors do that the sodium channel inactivation is voltage independent for the following reasons: *i*) species and channel difference; *ii*) structural difference in that the *shaker* potassium channel is assumed to consist of four monomers but the sodium channel of one larger monomer comprising four subunits; *iii*) as discussed above the findings by Aldrich et al. (1987) for sodium channel inactivation match our results quite well when taken literally. In our view the ball and chain hypothesis would be well compatible with voltage dependent inactivation if one assumes some form of mechanical coupling between such a cytoplasmic loop and the q_h generating voltage sensor that we postulate for inactivation. Indeed there is evidence for a structural connection between the internal side of the putative inactivation gate and the external side since α-scorpion toxin modifies inactivation from a receptor located at the outside of the channel (Tejedor and Catterall 1988). However, this suggestion needs further gating current studies in conjunction with molecular mechanical studies and, if possible, experiments with appropriately mutated sodium channels.

Conclusions

The isochronic analysis method introduced here represents a fresh approach to the interpretation and quantification of voltage dependent membrane processes. Its application requires only that accurate measurements of both ionic and gating currents be made from the same preparation under the same experimental conditions. In the present case the method was been applied to the study of the inactivation process for the squid Na channel, providing clear evidence for voltage dependence and a direct measure of the quantal charge involved. The findings corroborate those from the conventional Eyring-Boltzmann rate analysis and, most importantly, the method directly reveals the conditions under which rate analysis is valid, thus clearing up the controversy surrounding the very existence of voltage dependence for the inactivation step. An important consequence of this study is that it has shown a way for gating currents to be reinstated once more as part of the armament essential for the elucidation of the voltage dependent channel structure-function relations. And it would appear that gating current data used in conjunction with the new structural data from molecular biological studies will significantly accelerate the decipherment of the gating process in ion channels.

Acknowledgements. We thank the Director and staff of the Station Biologique de Roscoff, France for providing laboratory facilities and supplying squid, Professor R. D. Keynes for help in the experiments and Drs. J. M. Bekkers and R. Horn for helpful discussions about the manuscript. This work was supported by the Swiss National Science Foundation grant No. 3.143-0.85.

References

Aldrich RW, Stevens CF (1987) Voltage-depenent gating of single sodium channels from mammalian neuroblastoma cells. J Neurosci 7:418–431

Aldrich RW, Corey DP, Stevens CF (1983) A reinterpretation of mammalian sodium channel gating based on single channel recording. Nature (London) 306:436–441

Almers W, Armstrong CM (1980) Survival of K^+ permeability and gating currents in squid axons perfused with K^+-free media. J Gen Physiol 75:61–87

Armstrong CM (1981) Sodium channels and gating currents. Physiol Rev 61:644–683

Armstrong CM, Bezanilla F (1977) Inactivation of the sodium channel. II. Gating current experiments. J Gen Physiol 70:567–590

Augustine CK, Bezanilla F (1990) Phosphorylation modulates potassium conductance and gating current of perfused giant axons of squid. J Gen Physiol 95:245–271

Bekkers JM, Greeff NG, Keynes RD (1986a) The conductance and density of sodium channels in the cut-open squid giant axon. J Physiol (London) 377:463–486

Bekkers JM, Forster IC, Greeff NG, Keynes RD (1986b) Improvements in the recording of gating currents in the squid giant axon. J Physiol (London) 381:9P

Bekkers JM, Forster IC, Greeff NG (1990) Gating current associated with inactivated states of the squid axon sodium channel. Proc Natl Acad Sci USA 87:8311–8315

Berman MF, Camardo SS, Robinson RB, Siegelbaum SA (1989) Single sodium channels from canine ventricular myocytes: Voltages dependence and relative rates of activation and inactivation. J Physiol (London) 415:503–531

Bezanilla F (1985) Gating of sodium and potassium channels. J Membr Biol 88:97–112

Bezanilla F (1987) Single sodium channels from the squid giant axon. Biophys J 52:1087–1090

Bullock JO, Schauf CL (1978) Combined voltage-clamp and dialysis of Myxicola axons: behaviour of membrane asymmetry currents. J Physiol (London) 278:309–324

Catterall WA (1988) Structure and function of voltage-sensitive ion channels. Science 242:50–61

Chandler WK, Meves H (1970a) Sodium and potassium currents in squid axons perfused with fluoride solutions. J Physiol (London) 211:623–652

Chandler WK, Meves H (1970b) Evidence for two types of sodium conductance in axons perfused with sodium fluoride solutions. J Physiol (London) 211:653–678

Conti F, Stühmer W (1989) Quantal charge redistributions accompanying the structural transitions of sodium channels. Eur Biophys J 17:53–59

Cota G, Armstrong CM (1989) Sodium channel gating in a clonal pituitry cells. The inactivation step is not voltage dependent. J Gen Physiol 94:213–232

Forster IC, Greeff NG (1989) The quantal gating charge of sodium channel inactivation in the squid giant axon (*L. forbesii*). J Physiol (London) 418:11P

Forster IC, Greeff NG (1990) High resolution recording of asymmetry currents from the squid giant axon-technical aspects of voltage clamp design. J Neurosci Methods 33:185–205

Gilly WF, Armstrong CM (1980) Gating current and potassium channels in the squid giant axon of the squid. Biophys J 29:485–492

Gonoi T, Hille B (1987) Gating of sodium channels. Inactivation modifiers discriminate among models. J Gen Physiol 89:253–274

Greeff NG, Keynes RD, van Helden DF (1982) Fractionation of the asymmetry current in the squid giant axon into inactivating and non-inactivating components. Proc R Soc B 215:375–389

Greeff NG, Forster IC (1990) The quantal gating charge of Na channel inactivation obtained from gating currents and ionic current rate analysis. Biophys J 57:103a

Guy HR (1988) A model relating the structure of the sodium channel to its function. Current Topics Membrane Transport 3:289–308

Guy HR, Seetharamulu P (1986) Molecular model of the action potential sodium channel. Proc Natl Acad Sci USA 83:508–512

Hille B (1984) Ionic channels of excitable membranes. Sinauer, Sunderland, Mass

Hodgkin AL, Huxley AF (1952) A quantitative description of membrane current and its application to conduction and excitation in nerve. J Physiol (London) 117:500–544

Horn R, Vandenberg CA, Lange K (1984) Statistical analysis of single sodium channels. Effects of N-Bromoacetamide. Biophys J 45:323–355

Hoshi T, Zagotta WN, Aldrich RW (1990) Biophysical and molecular mechanism of *Shaker* potassium channel inactivation. Science 250:533–538

Keynes RD (1991) On the voltage dependence of inactivation in the sodium channel of the squid giant axon. Proc Soc B 243:47–53

Keynes RD, Rojas E (1976) Kinetics and steady state relationships between activation of the sodium conductance and movement of the gating particles in the squid axons. J Physiol (London) 255:157–189

Keynes RD, Greeff NG, Forster IC (1990) Kinetic analysis of the sodium gating current in the squid giant axon. Proc Soc B 240:411–423

Kosower EM (1985) A structural and dynamic molecular model for the sodium channel of *Electrophorus electricus*. FEBS Lett 182:234–242

Landowne D (1990) Chloramine-T alters the nerve membrane birefringence response. J Membrane Biol 113:123–129

Meves H, Pohl J-A (1990) A slow component in the gating current of the frog node of Ranvier. Pflügers Arch 416:162–169

Nagy K, Kiss T, Hof D (1983) Single Na channels in mouse neuroblastoma cell membrane. – Indications for two open states. Pflügers Arch 399:302–308

Noda M, Shimizu S, Tanabe T, Takai T, Kayano T, Ikeda T, Takahashi H, Nakayama H, Kanaoka Y, Minamino N, Kangawa K, Matsuo H, Raftery MA, Hirose T, Inayama S, Hayashida H, Miyata T, Numa S (1984) Primary structure of *Electrophorus electricus* sodium channel deduced from cDNA sequence. Nature 312:121–127

Noda M, Ikeda T, Kayano T, Suzuki H, Takeshima H, Kurasaki H, Takahashi H, Numa S (1986) Existence of distinct sodium channels from cloned cDNA. Nature 320:188–192

Rojas E, Keynes RD (1975) On the relation between displacement currents and activation of the sodium conductance in the squid giant axon. Phil Trans R Soc London B 270:459–482

Salkoff L, Butler A, Wei A, Scavarda N, Giffen K, Ifune C, Goodman R, Mandel G (1987a) Genomic organization and deduced amino acid sequence of a putative sodium channel gene in *Drosophila*. Science 237:744–749

Salkoff L, Butler A, Wei A, Scavarda N, Baker K, Pauron D, Smith C (1987b) Molecular biology of the voltage-gated sodium channel. Trends Neurosci 10:522–527

Scanley BE, Hanck DA, Chay T, Fozzard HA (1990) Kinetic analysis of single sodium channels from canine cardiac Purkinje cells. J Gen Physiol 95:411–437

Sigworth FJ, Neher E (1980) Single Na^+ channel currents observed in cultured rat muscle cells. Nature 287:447–449

Spires S, Begenisich T (1989) Pharmacological and kinetic analysis of K channel gating currents. J Gen Physiol 93:263–283

Stevens CF (1987) Sodium channel structure-function relations. In: Hille B, Fambrough DM (eds) Proteins in excitable membranes. Volume of The Society of General Physiology Series 41:99–108

Stimers JR, Bezanilla F, Taylor RE (1985) Sodium channel activation in the squid giant axon. Steady state properties. J Gen Physiol 85:65–82

Stühmer W, Conti F, Suzuki H, Wang X, Noda M, Yahagi N, Kubo H, Numa S (1989) Structural parts involved in activation and inactivation of the sodium channel. Nature 339:597–603

Swenson RP (1983) A slow component of gating current in crayfish giant axons resembles inactivation charge movement. Biophys J 41:245–249

Tejedor FJ, Catterall WA (1988) Site of covalent attachment of α-scorpion toxin derivatives in domain I of the sodium channel subunit. Proc Natl Acad Sci USA 85:8742–8746

Vandenberg CA, Horn R (1984) Inactivation viewed through single sodium channels. J Gen Physiol 84:535–564

White MM, Bezanilla F (1985) Activation of squid axon K^+ channels: Ionic and gating current studies. J Gen Physiol 85:539–554

Yamamoto D, Yeh JZ, Narahashi T (1984) Voltage-dependent calcium block of normal and tetramethrin-modified single sodium channels. Biophys J 45:337–344

Yue DT, Lawrence JH, Marban E (1989) Two molecular transitions influence cardiac sodium channel gating. Science 244:349–352